INSTITUTE OF PHYSICS PUBLISHING PHYSICS IN MEDICINE AND BIOLOGY

Phys. Med. Biol. **51** (2006) R117–R137 doi:10.1088/0031-9155/51/13/R08

REVIEW

Positron emission tomography

Gerd Muehllehner and Joel S Karp

Department of Radiology, University of Pennsylvania, 3400 Spruce Street, Philadelphia, PA 19104, USA

Received 1 February 2006, in final form 23 April 2006
Published 20 June 2006
Online at stacks.iop.org/PMB/51/R117

Abstract

The developments in positron emission tomography (PET) are reviewed with an emphasis on instrumentation for clinical PET imaging. After a brief summary of positron imaging before the advent of computed tomography, various improvements are highlighted including the move from PET scanners with septa to fully 3D scanners, changes in the preferred scintillators, efforts to improve the energy discrimination, and improvements in attenuation correction. Time-of-flight PET imaging is given special attention due to the recent revival of this technique, which promises significant improvement. Besides technical instrumentation efforts, other factors which influenced the acceptance of clinical PET are also discussed.

Introduction

In this paper we review some of the historical developments in positron emission tomography (PET), concentrating on the major events and factors influencing instrumentation development and the acceptance of PET as a clinical tool. Other areas such as radiopharmaceuticals and organizational and societal factors are touched upon as they influenced the direction and speed of instrumentation development. The perspective is largely a personal one without a serious attempt to be all-inclusive, particularly regarding the many contributions made by a large number of investigators in this dynamic field. It is intended to show the development of the technology used in current PET scanners rather than a history of the people responsible for it. Another history of PET from a different perspective was published recently by Nutt (2002).

PET is a nuclear medicine technique which requires the combination of a number of factors before any PET procedure can become an important clinical tool. Indeed, PET as a whole could not become a clinical specialty until the 'typical' medical facility saw the need to offer PET as part of their diagnostic procedure capability. The factors we consider critical are:

(1) *The necessary radioisotope has to be available on a daily basis*. In the early phases of PET it was considered essential that a PET facility have its own cyclotron, which in our opinion significantly delayed the introduction of PET as a clinical tool. More reasonably,

the requirement is the availability of a radioisotope with a long enough half-life to allow at least regional distribution, but a short enough half-life to minimize the radiation exposure to the patient. This requirement was fulfilled with fluorine-18 (F-18), which is tagged to fluorodeoxyglucose (FDG) and which now dominates clinical PET. Currently there are several companies providing reliable distribution of FDG throughout the country.

(2) *An imaging device must give good performance for the isotope of choice*. Just as in single-photon nuclear medicine this combination is the Anger camera and technetium-99m, so in PET this combination is the modern day PET scanner and F-18. Further, the instrument's performance is optimized to perform well at activities corresponding to the allowable injected dose for clinical studies, which in the case of FDG is 10–15 mCi.

(3) *The combination of a radiopharmaceutical and a patient population for which the PET scan provides significant diagnostic information which is not readily available with other techniques*. It is surprising that this last step took several years to identify. PET was first used to study the brain, without ever finding that significant application which transformed PET from a research tool to a clinical tool. The second area which was investigated extensively was cardiac viability using F-18 fluorodeoxyglucose and N-13 ammonia to identify a mismatch between metabolism and blood flow as an indicator of tissue viability, which is now used relatively little in clinical practice. Finally, the use of FDG to indicate increased metabolism primarily in tumours provided the applications combining a large patient population and significant impact of PET procedures on patient treatment and prognosis which justified reimbursement by third party payers and which moved PET from the research arena to clinical practice. This long and tedious process explains why PET languished for years during a period in which CT and MRI moved quickly from early laboratory experiments to wide-spread clinical use.

Our own motivation to develop PET instruments, together with their reconstruction algorithms and data correction methods, stems largely from the limited opportunity to significantly improve single-photon imaging. In many ways, the Anger scintillation camera is ideally suited to image the 140 keV radiation from Tc-99m: the relatively thin NaI(Tl) crystal used in the Anger camera stops close to 100% of the gamma-rays, the spatial resolution of the detector can be made good enough to have little influence on the system performance and this performance can be achieved without undue technical difficulties and expense. The main limitation becomes the collimator: the collimator limits both spatial resolution and sensitivity, requiring a compromise between these two essential performance parameters in a way that makes significant improvements in the imaging performance extremely difficult. PET, on the other hand, decouples those two performance parameters, allowing the development of high-resolution instruments with high sensitivity. Particularly in view of the fact that nuclear medicine images have always suffered in image quality when compared to other medical imaging modalities such as CT and MRI (resulting in the fact that nuclear medicine was sometimes referred to as unclear medicine by its detractors), it seemed essential to improve the image quality of nuclear medicine images in order to improve the diagnostic information which can be derived from them. This in no way is intended to downplay the importance of the choice of the appropriate radiopharmaceutical, which primarily determines the contrast and visualization of the intended structures and provides functional information which is often not available from largely anatomic imaging techniques such as CT and MRI.

PET, by its very nature of imaging, requires the use of isotopes which are different from the single-photon emitters in current use in nuclear medicine. This also implies that the chemistry and choice of radiopharmaceuticals must be different. A number of review articles e.g. Stoecklin (1995) contain long lists of potential radiopharmaceuticals based on the four or five most common positron-emitting radioisotopes, making it difficult for the reader to

Table 1. Abbreviated list of positron-emitting isotopes of potential interest in PET imaging.

	O-15	N-13	C-11	F-18	Rb-82	Ga-68	Cu-62
Half-life	2 min	11 min	20 min	110 min	75 s	68 min	9.7 min
Availability	On-site cyclotron	On-site cyclotron	On-site cyclotron	Cyclotron, regional distribution	Generator Sr-82/Rb-82	Generator Ge-68/Ga-68	Generator Zn-62/Cu-62

judge the probability that any of them will reach clinical use. Table 1 lists the rather short list of radioisotopes that can be considered for PET imaging (other impure positron emitters such as I-124 and Y-86 are also being investigated, primarily for radioimmunotherapy). The short half-life of O-15, N-13 and C-11 make clinical applications quite difficult or impossible in a large number of institutions. The need for an on-site cyclotron is apparent; in addition, the short half-life requires a very rapid conversion from the isotope to the appropriate radiopharmaceutical, which is often difficult to achieve, and also requires a scheduling accuracy (availability and readiness of both patient and imaging instrument) which places an additional burden on achieving a successful study. The generator-produced isotopes listed in table 1 have so far not yielded a clinical procedure which fulfils the requirement listed above for a radiopharmaceutical and a patient population which provides significant diagnostic information not readily available with other techniques. This leaves F-18 as the most likely candidate for any widely used radiopharmaceutical; indeed dozens of F-18 labelled tracers are being tested for research studies Stoecklin (1995).

At the present time F-18 FDG is used almost exclusively in clinical procedures as a marker of increased metabolism, which sometimes has the disadvantage that it is not very specific. This review is therefore the story of PET using FDG, primarily in whole-body tumour imaging. While we hope that other radiopharmaceuticals and applications will broaden the appeal of PET, the current success of PET is based almost exclusively on FDG whole-body imaging and this is reflected in the type of PET scanners currently in use.

Early history

The potential of positron imaging and the value of eliminating the collimator was recognized by the early developers of nuclear medicine instrumentation, long before the advent of reconstruction algorithms which could allow the generation of transverse sections from data covering a large number of angles. G Brownell and his group developed a family of instruments over several decades that nicely demonstrate the evolution of PET first from dual planar detectors (Brownell *et al* 1969) working in coincidence and providing longitudinal tomographic images, progressing from there to rotating detectors and using transverse reconstruction algorithms to obtain transverse sections and finally to complete circular stationary detector arrangements, first with a single slice (Burnham *et al* 1983) and subsequently using an increased number of transverse slices (Burnham *et al* 1985). Hal Anger also worked on positron imaging almost as soon as he developed the single photon Anger camera (Anger 1966). His dual detector PET scanner was made commercially available for a brief period by Nuclear Chicago Corp, but early clinical data quickly pointed out the main problem with PET imaging: while the elimination of the collimator increased the photon flux hitting the detectors by more than an order of magnitude relative to single photon imaging, the fraction of event which are found in coincidence is of the order of 1%, therefore requiring a high singles countrate capability to achieve an acceptable coincidence rate.

It is also interesting to note that time-of-flight (TOF) imaging was a gleam in the eyes of these early investigators (Brownell *et al* 1969), leading Brownell to conclude in 1969 that with the then state-of-the-art scintillators and photomultiplier tubes, TOF—which increases in benefit as the object size increases—was useful for elephants, but not yet humans. TOF then went through a period of revival in the 1980s and is only now being revived for a third time, as will be described in more detail below.

The instrumentation efforts before about 1975 suffered not only from a lack of knowledge about transverse section reconstruction methods, but also from a severe lack of computing power. Longitudinal tomographic images were often obtained with dedicated electronic processing methods instead of superposition of data using digital techniques, since even a single image with a 64 $\times$ 64 matrix was considered to require a large amount of storage space. At the time the primary potential clinical application was bone scanning with F-18 and some of the early positron bone scans were of stunning quality by the standards of that time, demonstrating the ability of PET to combine excellent spatial resolution with high sensitivity.

Early efforts to achieve transverse section images in nuclear medicine relied on iterative methods (Muehllehner and Wetzel 1971, Kuhl *et al* 1973), but this changed rapidly with the introduction of x-ray computed tomography and the filtered backprojection technique. This allowed a series of PET scanners to be developed at a number of academic institutions (Ter-Pogossian *et al* 1978, Phelps *et al* 1976, Burnham *et al* 1985, Bohm *et al* 1978, Senda *et al* 1985, Cho 1983, Derenzo *et al* 1981, Wong *et al* 1984), using first NaI(Tl) in a hexagonal arrangement (Phelps *et al* 1976), a 1-to-1 crystal-to-photomultiplier tube (PMT) coupling and involving transverse scanning and wobbling motions, finally leading to the use of BGO in a circular arrangement operating in stationary mode (Thompson *et al* 1979, Cho and Farukhi 1977). It also changed the approach of our own efforts starting with multiple longitudinal planar images to the reconstruction of transverse section using dual rotating detectors, culminating in the development of a fully 3D acquisition (Muehllehner *et al* 1976) and reconstruction (Colsher 1980) in the late 1970s. After the introduction of transverse section reconstruction using filtered backprojection, PET imaging entered a period of rapid advancement and increased use in a number of leading research institutions, particularly because this also coincided with the development of FDG (Reivich *et al* 1979) which created an opportunity to study brain function in a way that was impossible up to that point. In subsequent sections we will emphasize the evolution of PET starting in the mid-1970s initially with an emphasis in a large number of research institutions on functional brain imaging followed many years later by a transition to clinical practice and whole body tumour imaging.

Instrumentation concepts and developments

Crystal-to-PMT encoding

Early PET scanners used relatively large scintillation crystals and coupled one crystal to one PMT in a single slice (Phelps *et al* 1976, Bohm *et al* 1978, Cho *et al* 1983). This significantly limited both the spatial resolution (which required many small crystals) and the sensitivity (which required even more crystals and PMTs to image many slices simultaneously) unless one was willing to increase the complexity of the instrument significantly. Efforts started almost immediately to couple more than one crystal to one PMT using a variety of methods including the use of crystals with differing decay times (Eriksson *et al* 1985), encoding the axial position using Anger logic (Ter-Pogossian *et al* 1978), and triggering more than one PMT per event (Ter-Pogossian *et al* 1978). Most of these methods achieved an encoding ratio of 2:1 or 4:1 crystals per PMT. Since our background was related to the Anger scintillation camera,

it was a natural evolution to build PET scanners using the large encoding ratio typical of the Anger camera of more than 200 resolution elements per PMT. An Anger camera uses a thin (3/8 inch) continuous crystal to achieve 4 mm spatial resolution using an array of 65 mm PMTs. In contrast, PET detection of 511 keV gammas requires a thicker (1 inch) crystal, which can achieve 6–7 mm spatial resolution with 65 mm PMTs. Over the years, methods of crystal identification converged to the point that current encoding ratios of 50:1 are not unusual. One of the major steps in that direction was the development of the block detector (Casey and Nutt 1986). This represented a convenient building block and was a more serviceable solution than the more continuous solution of (Burnham *et al* 1985). The number of resolution elements which can be resolved depends to a large degree on the amount of light being emitted by the scintillator. Since most discrete detector PET scanners used BGO (see below for a discussion of material), which has relatively low light output, it was difficult to achieve an encoding of more than 8 × 8 crystal array on a 2 × 2 PMT array leading to a crystal/PMT ratio of 16:1. This is in sharp contrast to the encoding ratio achieved in our NaI(Tl) based PET scanners, where we typically achieved 6–7 mm detector resolution with a continuous detector and 65 mm diameter PMTs leading to a 100:1 ratio or finally 4 mm detector resolution with a pixelated detector and 50 mm diameter PMTs, again leading to an encoding ratio of >100:1 (Perkins *et al* 2003). Ultimately, the use of continuous NaI(Tl) detectors was abandoned in 2003 in favour of discrete crystal configurations. The combination of thick crystals and continuous scintillators allowed light to spread too far in the crystal to still achieve good spatial resolution in spite of the high light output of NaI(Tl). In addition, the limited stopping power of NaI(Tl) resulted in an inferior singles-to-coincidence ratio and thus limited the maximum countrate capability of the scanners. While going to discrete NaI(Tl) crystals (Perkins *et al* 2003) solved the first problem, the problem of a limited maximum countrate capability with NaI(Tl) was never solved adequately.

To achieve higher countrate capability, a faster scintillator is required. For example, we achieved similar 4 mm detector resolution with the lower light output scintillator GSO configured in a pixelated detector with 39 mm diameter PMTs, leading to an encoding ratio of >50:1 (Surti *et al* 2000). In parallel, the development of LSO and LYSO scintillators, which have significantly higher light output than BGO finally combined the high stopping power desired with a high enough light output to achieve high encoding in a block design, for example a 13 × 13 crystal array in a 2 × 2 PMT block, resulting in an encoding ratio of 42:1. The goal of all of these efforts is to allow the designers to use more and smaller crystals to achieve both better spatial resolution and higher sensitivity without increasing the complexity of the instruments beyond reasonable limits in terms of the number of PMT and electronic processing channels. The reason for the relationship between light output and achievable encoding ratio is simple: the PMTs must detect a statistically significant amount of light in order to allow the Anger centroid finding algorithm to identify the locus of the light emitted with enough accuracy to identify an individual crystal with reasonable probability. The more light is received by each PMT, the more accurately the centroid can be determined. In addition, the amount of light being detected per PMT must change as a function of location of the impinging gamma-ray; this is achieved by controlling the light spread. A higher crystal to PMT encoding ratio does have the disadvantage that the countrate per PMT increases leading to increased deadtime; fortunately the trend towards higher encoding ratios coincided with a shift towards faster scintillators, negating the loss in countrate capability.

How light is directed to the PMTs involved in positioning an event can be achieved by a number of different techniques. In an Anger scintillation camera, a lightpipe is used to allow the light from the scintillation crystal to reach a certain number of PMTs and to affect the amount of light reaching each PMT as a function of origin of the light. In a PET scanner using

a block design this can be achieved by either using a lightpipe with slots cut into the lightpipe, which was replaced a short time later by slots cut directly into a block of BGO. The relative light distribution is controlled by varying the depth of the slots cut into the crystal block. Alternately, the light passing from one crystal to neighbouring crystals can be controlled by changing the reflectors between the crystals (Wong *et al* 1994). In our designs, which avoid the use of individual blocks, the light spread is controlled by optimizing the thickness of a lightpipe to share the light among seven PMTs in a close packed hexagonal arrangement (Karp *et al* 2003).

From 2D to 3D

Practically all early PET scanners used septa between the transverse slices to reduce the scatter from the patient. This was necessary, since the energy resolution was typically quite poor. This is particularly true of BGO scanners due to the low light output of the material. Furthermore, the coupling of many crystals to a quadrant arrangement of PMTs further increased the variation of light collection from different crystals and typically resulted in poor light collection from crystals in the corners of a block (Cherry *et al* 1995). Since our own experience came from single photon imaging, where the Anger camera already achieves uniform 10% energy resolution even at a low energy of 140 keV, it was natural to use those techniques to design a PET scanner with a nearly uniform energy resolution. What little variation in light collection exists in a continuous detector coupled to a hexagonal arrangement of PMTs was further reduced through the use of digital spatially varying energy correction as is customary in single-photon imaging. This results in improved energy resolution and allowed us to use fully 3D data collection and raise the level of energy discrimination to reduce patient scatter to an acceptable level. This is more easily achieved in brain imaging, since in that case not only is the object diameter smaller than in body imaging, but the radiation from outside the axial field-of-view is also well shielded. In 1991 the first BGO-based PET scanners with retractable septa were introduced (Mazoyer *et al* 1991, Spinks *et al* 1992) leading to numerous publications e.g. Lartizien *et al* (2002) investigating the trade-off between the beneficial increase in sensitivity resulting from the elimination of the septa and the detrimental increase in scattered radiation. Since in 2D, the septa are used to sharply reduce the scattered radiation, energy resolution is less important, while high crystal stopping power is more important due to the reduction in sensitivity of the septa; in 3D on the other hand good energy resolution and the use of a high energy discrimination threshold become essential (Karp *et al* 1991a). Figure 1 shows the relationship between energy threshold, object diameter and scatter fraction demonstrating the importance of energy resolution. The energy threshold is related to the energy resolution (see table 1): the energy threshold can be raised until the threshold starts to eliminate photopeak events and the resulting loss of true sensitivity outweighs the benefit of reduction in scattered events. The thresholds in commercial scanners have been raised over time (accounting for the wide range of thresholds shown in figure 1), as the materials and techniques have improved and as the importance of better scatter rejection has been appreciated for 3D imaging. Note that the LaBr in a 3D scanner results in about the same scatter fraction as a BGO scanner in 2D mode. The effect of object diameter will be further discussed in a later section. With the move away from BGO to materials with better energy resolution, such as GSO, LSO, LYSO and LaBr, the trend towards septa-less fully 3D scanners will continue.

Choice of scintillator material

It is important to realize that the critical design parameters change significantly between a 2D PET scanner and a 3D PET scanner. Therefore simply removing the septa was only a

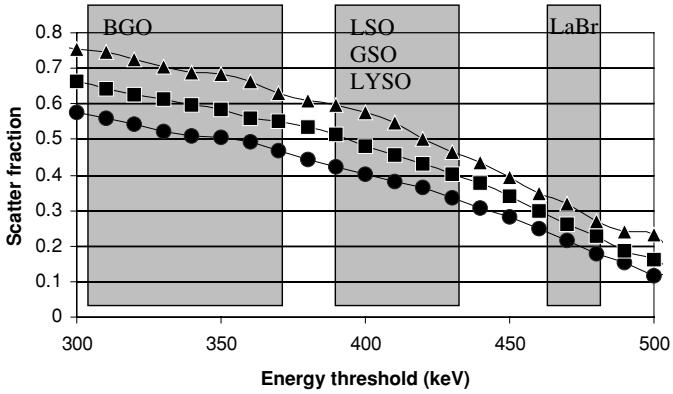

Figure 1. Scatter fraction as a function of energy threshold for a 20 cm (circles), a 27 cm (squares) and a 35 cm (triangles) diameter cylinder, 70 cm long in a typical 3D scanner (computer simulation assumes detector ring diameter = 85 cm, axial field-of-view = 18 cm, courtesy S Surti, U Pennsylvania). The range of energy thresholds for various scintillators are indicated with the upper range typically associated with more recently available scanners.

Table 2. Physical parameters important in 2D versus 3D imaging for various scintillators.

	Parameter important for 2D	Parameters important for 3D	
	Stopping power (attenuation length, cm)	System energy resolution (%)	Decay time (ns)
BGO	1.05	18–25	300
NaI(Tl)	2.88	10–12	230
GSO	1.43	12–18	60
LSO/LYSO	1.16	12–18	40
LaBr(Ce)	2.13	6–7%	27

first step. In a 2D scanner, the roughly five-fold decrease in sensitivity of the septa must be compensated as much as possible by selecting a detector material with the highest possible stopping power. Since the countrate impinging on the detector is also reduced by the septa, the decay time is less important. In 3D in the other hand, energy resolution—to reduce the scattered radiation, and decay time—to be able to handle the higher data rates, become most important while stopping power is reduced in importance. The scintillators used in PET scanners are summarized in table 2 and the shift from BGO and NaI(Tl) to GSO, LSO, LYSO and LaBr can be appreciated as scanners move from 2D to 3D acquisition. Since our group has always worked on 3D scanners, we have preferred scintillators with the best energy resolution (e.g. Na(Tl) and LaBr(Ce)), while groups with more experience with 2D imaging have considered stopping power the most important parameter.

One parameter that is typically not discussed in the scientific literature is the effect of the price of the scintillator on design. In most commercial PET scanners the cost of the scintillator material represents 30–50% of the material cost of the scanner. This severely impacts the amount of material that can be used without making the scanner prohibitively expensive. For example, NaI(Tl) is typically cheaper by a factor of 2 compared to BGO, so that is was possible to use a 30 mm thick scintillator in a PET scanner with an axial FOV of 25 cm, while BGO scanners never took the step of increasing the axial FOV beyond

Table 3. Measured peak count rates for 70 cm long cylinders of different diameters. Values (relative to measurements for 35 cm phantom) are averaged between two scanners operating in 3D (*Advance* by General Electric and *Allegro* by Philips).

Object diameter (cm)	Relative attenuation	Peak trues ratio	Peak NEC ratio	Peak NEC density ratio
20	4.3	3.4	6	18
27	2.2	2	2.7	4.5
35	1	1	1	1

15–16 cm. GSO and LSO/LYSO started out costing significantly more than BGO, which inhibited their use early on. As manufacturing problems were solved, the price of these scintillators was reduced and their utilization became more wide-spread. At the present time, LaBr is still not in routine large-scale production, which inhibits the use of this scintillator in a commercial scanner in spite of its excellent energy resolution, short decay time and superb coincidence resolving time. However, these properties make it an ideal candidate for a time-of-flight (TOF) PET scanner and help motivate the continuing development of this scintillator.

The heavy patient problem

Countrate capability of PET scanners is typically measured using a 20 cm diameter cylinder according to the NEMA standard. This was chosen 15 years ago as the standard diameter (Karp *et al* 1991a) since it was considered to be a compromise between a brain and a body size, although the more recent NU 2 standard extends the length of the phantom to 70 cm to better represent the body (Daube-Witherspoon *et al* 2002). The data from these measurements lead to the conclusion that at activity concentrations typically encountered in clinical FDG studies (approximately 0.1 μCi cm^{-3} 1 h after the injection of 10 mCi of activity), count losses are minimal and the scanner is being used well below the level where randoms and deadtime effects are significant. The situation, however, changes significantly with body size or girth. We have suggested using larger phantoms to assess scanner performance and to better represent a range of body sizes (Surti and Karp 2004); note that 20 cm diameter corresponds to a 25 inch (63 cm) waist, which is very thin, while a 27 cm diameter cylinder is equivalent to a patient with a 33 inch (85 cm) waist, and 35 cm corresponds to a 43 inch (110 cm) waist, which is a better representation of heavy patients but still far from the upper limit of what we see in the clinic. Most clinicians with PET experience know that image quality degrades rapidly as the patient weight increases. The primary cause is the increased attenuation in larger patients as shown in table 3.

Table 3 shows that as the diameter of the object is increased from 20 cm to 27 or 35 cm diameter, the true coincidences decrease in direct proportion to the increased attenuation (the measured values in table 3 are affected by deadtime leading to a reduction in the ratio for the measured values). The reduction in true coincidences is, however, accompanied by an increase in scattered radiation and an increase in random coincidences as we move from a 20 cm diameter cylinder to 27 or 35 cm. This is reflected in the NEC values also shown in table 3. The difference in peak NEC between a 20 cm and a 35 cm phantom is approximately a factor of 6. In addition, the counts are distributed over a larger volume in a heavy patient; this means that it is more meaningful to look at count *density* rather than total counts. Table 3 shows the NEC count density as a function of phantom diameter, showing a factor of 18

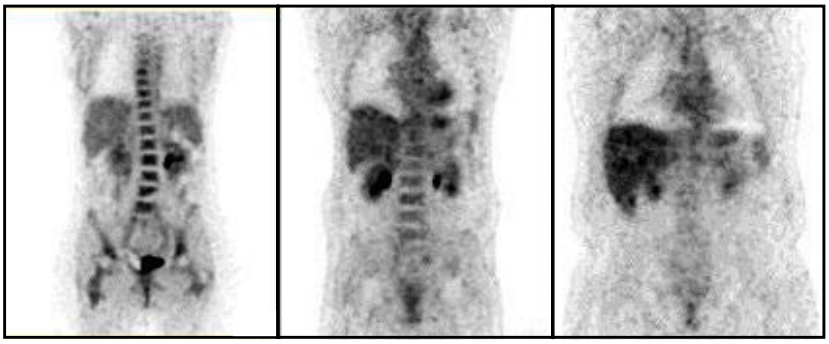

Figure 2. Coronal images for a slim patient (58 kg, left image), 'average' patient (89 kg, middle image) and a heavy patient (127 kg, right image) demonstrating the deterioration in image quality as a function of patient size. Data from Philips *Allegro* scanner at U Penn.

in count density between the 20 cm and the 35 cm phantom. Dealing with image quality of heavy patients was not addressed per se in the literature until quite recently, since most instrumentation improvements will benefit all patient images. As the image quality has improved over the years, it becomes more challenging to improve the diagnostic accuracy for slim patients through instrumentation efforts alone, since diagnostic accuracy is also determined by the relative uptake of the radiopharmaceutical. In heavy patients, however, limitations in the instrumentation are still quite significant. Figure 2 shows the effect on image quality in clinical scans, demonstrating the degradation in image quality with body weight. It is important to note that incorporating TOF information in the reconstruction will benefit heavy patients much more than slim patients; this strongly motivates our renewed investigation of this technique.

Algorithms and corrections

Filtered backprojection was the obvious initial choice to reconstruct PET images, since this was the standard method for CT and SPECT. Iterative algorithms have the disadvantage of being more computationally intensive and that the image changes both qualitatively and quantitatively as the number of iterations and the relaxation parameter(s) change. Since PET was largely if not exclusively used for research studies in the early years of PET, quantitative accuracy was critical. This state-of-affairs did not change significantly until after attenuation correction through measured transmission scans became more generally used. As will be demonstrated below, the image quality improvement, when iterative algorithms are used for both the emission and the transmission scans, is so overwhelming, that iterative algorithms became the method of choice in attenuation corrected clinical PET imaging once the computing power became sufficient to make iterative reconstruction practical.

Attenuation correction

A number of corrections are typically performed on PET data both before and/or during the reconstruction process. These include normalization, scatter correction, randoms correction and attenuation correction. Of these corrections, attenuation correction makes by far the biggest change in the quantitative values as well as the visual appearance of the images. This is due to the fact that attenuation can easily be a factor of 10 or greater through the centre of

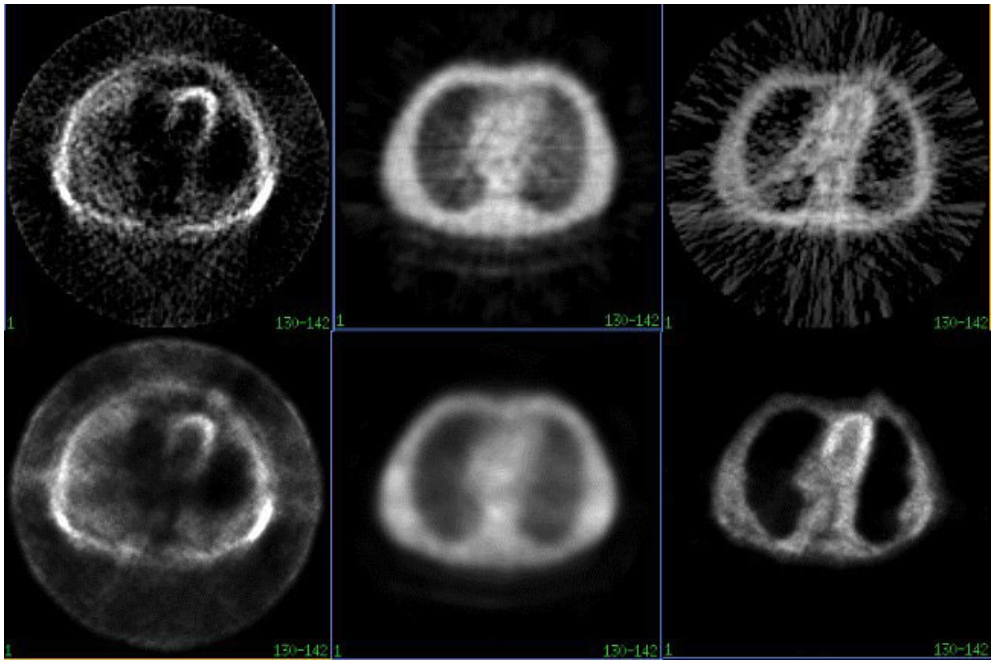

Figure 3. Same data set reconstructed with filtered back-projection (top row) and iterative reconstruction (bottom row). Left column shows uncorrected emission images, middle column shows transmission images, right column shows attenuation corrected emission images. Data from ADAC UGM *C-PET* scanner at U Penn.

the body. Without attenuation correction there is a significant variation in reconstructed image density across the FOV, with the lowest intensity in the centre of the image.

Originally attenuation correction was performed by inserting a thin, hollow cylinder of a positron emitting activity around the patient before the radiopharmaceutical was injected. This required the patient to be immobilized during the transmission scan, the radioisotope uptake period—typically 45 min—and the actual scan. This procedure was complicated enough to severely restrict the usefulness of the technique and most clinical whole-body scans were performed for over a decade without transmission imaging. The ability to perform post-injection transmission scans was a major step forward (Carson *et al* 1988). This was achieved by replacing the ring of activity by a rotating line source. Since the location of the line source was known as it rotated, it was possible to differentiate between most of the emitted radiation and the transmitted radiation. Nevertheless, the transmission scan still required as long a time as the emission scan to acquire and the resulting images were quite noisy. This led to the conclusion that transmission corrected emission scans did not improve diagnostic accuracy (Bengel *et al* 1997). These publications used a filtered back-projection algorithm to reconstruct both the emission and the transmission images. Figure 3 shows the effect that an iterative algorithm has on a data set compared to a filtered back-projection method. The reduction in noise and increase in useful information is striking.

Singles transmission

One of the major problems with transmission imaging using a coincidence technique in order to differentiate between emitted and transmitted activity is the high countrate impinging on the

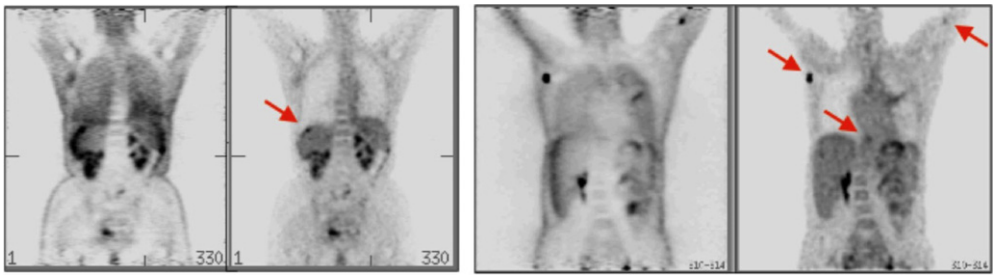

Figure 4. Comparison of whole-body scans (coronal views) without attenuation correction (1st and 3rd images) and with attenuation correction (2nd and 4th images). Data from Philips *Allegro* scanner at U Penn.

detectors closest to the transmission source. Due to the attenuation in the patient's body the coincidence fraction is quite low, leading to both high singles rates in the near detectors and long acquisition times to get adequate data quality in the transmission images. This situation can be improved if the transmission source is replaced with a singles emitter of higher energy than the 511 keV from the patient. This allows the differentiation between emitted and transmitted radiation to be performed on the basis of the energy of the detected events, so that post-injection transmission measurements are possible. The fact that the singles source can be shielded towards the near detectors allows the amount of activity in the transmission source to be increased substantially. This method was investigated for both NaI(Tl) based (Karp *et al* 1995) as well as BGO based (Yu and Nahmias 1995) PET scanners using Cs-137 as the transmission source with an energy of 662 keV, but the poor energy resolution of BGO prevented the method from being used widely. Figure 4 shows representative coronal images from two studies, each without attenuation correction (AC) and with AC. Note that the relative activity uptake in the lesions is more reliably determined with AC. The attenuation coefficients are generated from a singles transmission scan with an acquisition time of 'only' 6.5 min for the whole scan, which is a small fraction of the emission scan of about 30 min.

CT attenuation correction

The introduction of a combined PET/CT scanner changed the practice of clinical PET within just a few years—currently all new PET scanners sold are combined PET/CT scanners. Transmission scanning using radioisotopes is quickly being phased out since the low dose CT scan results in a significant reduction in the total transmission scanning time (to less than 1 min), particularly for multi-slice CT scanners. Although the idea seems straight-forward, the overall effort to generate the attenuation corrected image with CT without artefacts is still on-going and summarized nicely in Alessio *et al* (2004). The technical challenges were/are the following: (1) converting the CT transmission scan from low energy to 511 keV, which requires a nonlinear transformation. (2) Reduction of artefacts due to patient, cardiac and respiratory motion. The long acquisition times of PET prohibit breath holding, while most CT scans were performed during breath holding, resulting a attenuation artefacts, particularly near the dome of the liver. (3) Estimation of attenuation for parts of the patient outside the transverse field-of-view (FOV) of the CT scan. Most CT scanners have a transverse FOV of 50 cm, which is less than the FOV of the PET scanner and also less than the extent of some patients. (4) Reduction of artefacts due to injected contrast agents and metal implants or prostheses, requiring a more sophisticated segmentation algorithm.

The impact of the arrival of PET/CT goes well beyond attenuation correction and will be discussed in more detail later in this chapter.

Coronal views

Early whole body scans could only be viewed as a large number of transverse slices; for a 100 cm long scan with 5 mm thick slices, this meant looking at 200 individual slices, each of which had few landmarks. It was not until 1992 (Dahlbom *et al* 1992) that whole body scans were routinely displayed in coronal views. The impact on the ease of clinical interpretation of PET scans cannot be underestimated. Not only did the number of views to be viewed decrease significantly, but in addition, coronal views allow one to visualize important anatomic landmarks, which aid significantly in the interpretation of scans. In addition, the ability to add slices as part of the viewing process allowed the display of images, which had reduced statistical fluctuations without reducing the edge definition of structures. Today, however, with improved image quality of transverse sections (see, e.g., figure 3), and with more radiologists reading PET, the utilization of coronal sections is not as crucial to clinical interpretation. Nevertheless, the ability to view transverse, sagittal and coronal images on the same screen combined with the use of cross-hairs to provide a 3D reference point eases the task of interpretation and registration with anatomical images such as CT (or MR) for those situations where the data are acquired on separate instruments. Certainly, the interpretation of PET scans is more time consuming and difficult than many other nuclear medicine diagnostic imaging tasks, such as Tc-99m bone scans.

The reconstruction challenge

As the spatial resolution of PET scanners has improved, mostly by using more and smaller crystals, the number of pixels to represent the image has also increased. It is common practice to display transverse whole-body images in 128×128 format. If each slice has a thickness of 4 mm, then a typical 100 cm long whole body scan has $128 \times 128 \times 250 = 4$ million pixels. Unfortunately, the number of pixels in the acquired data matrices is significantly larger (by up to two orders of magnitude), since the number of lines of response (LOR) increases as the square of the number of crystals. In fact, current clinical PET scanners typically have more LORs than the number of counts (100–200 million) acquired in a whole body scan. How to reconstruct a 3D image volume using such sparse data has been and remains a challenge. In our effort to improve PET image quality, the effect of the reconstruction algorithms and data correction methods are often not given enough attention, since the benefits of improved reconstruction methods are harder to quantitate than the more basic physical parameters associated with the physical detector characteristics.

The move to clinical PET

PET development was started well before the advent of MRI, but MRI became widely used decades before PET and PET still has not achieved the same impact on medical practice as MRI in spite of the significant metabolic information contained in PET scans. PET has had a difficult time establishing itself as a routine clinical tool among diagnostic imaging modalities. This was not as a result of lack of dedication among those investigators that were directly associated with it, but was due to the confluence of a number of factors.

Area of application

After the first successful PET scan using FDG in 1976 (Reivich *et al* 1979), one would have expected PET to be applied quickly to tumour imaging due to the known increased metabolic rate of tumours and the fact that FDG is a marker of glucose metabolism. However, the first

several PET centres that were funded by NIH concentrated on studying brain metabolism and brain function. Within a few years cardiac imaging received wide-spread attention using FDG and N-13 ammonia to study flow-metabolism mismatch as an indicator of tissue viability. Neither of these applications led to significant clinical applications today. After DiChiro *et al* (1982) in 1982 showed that tumour metabolism was associated with prognosis in brain tumours, it took a long time for researchers to fully exploit the clinical utility of tumour imaging.

What is a PET centre?

The early PET centres were primarily funded by the National Institutes of Health (NIH) and/or the Department of Energy (DOE) and needed both a scanner as well as an on-site cyclotron to generate the necessary isotopes. Furthermore, a radiochemistry laboratory was necessary to manufacture radiopharmaceuticals. The typical staff of such a PET centre consisted of somewhere around ten people including a physicist for the scanner and data evaluation, a cyclotron engineer, a cyclotron operator, a radiochemist with a technician, a nuclear medicine technologist, a physician and an administrator. To establish such a PET centre took first several years to arrange the funding and the space and then an additional year to staff the centre and progress to the point where the facility was fully licensed and functioning (Hawkins *et al* 1991). After it became more difficult to obtain NIH funding for a PET centre, a number of academic institutions funded a PET centre, but the operating expenses continued to be a money drain for these institutions. During this period (1985–1998) PET grew very slowly, also resulting in financial problems for the scanner manufacturers. The deficit at CTI had to be covered by Siemens, while General Electric became so disenchanted with PET that they briefly considered outsourcing the design and manufacturing of PET scanners to Positron Corporation. Positron Corporation itself went through several stages of refinancing by venture capital groups. UGM Medical Systems managed to barely stay financially healthy by keeping the size of the company small and funding the effort through grants (Small Business Innovative Research (SBIR) grants) and by providing consulting services to other companies. The high cost of entry into the PET business had another unfortunate side effect: since most nuclear medicine departments had little chance to convince their hospital administration to fund such a PET centre, PET received little support from within the Society of Nuclear Medicine and its membership. Instead the effort to bring PET to the clinical stage by obtaining FDA approval for FDG and reimbursement for tumour studies was spearheaded by the Institute of Clinical PET (ICP) and the leadership and personal effort of Michael Phelps.

Factors influencing the growth of PET

In the late 1990s, PET had a sudden spurt of growth to which a number of factors contributed. These are (1) FDA approval of FDG and reimbursement by HCFA (1998), (2) distributed FDG, (3) hybrid SPECT/PET scanners, (4) mobile PET scanners. To some extent these factors are interrelated. In order to allow a PET centre to be established without the expense of a cyclotron and the associated staffing, it was necessary to have local pharmacies distribute FDG from their cyclotron. This, however, only made economic sense after enough customers lived within a reasonable distance from the radiopharmacy. In 1995 ADAC introduced the MCD dual detector SPECT/PET scanner that was developed in cooperation with UGM Medical Systems. Within 18 months the total number of MCD systems sold equalled the number of dedicated PET scanners sold within the previous 10 years within the United States, thereby significantly increasing the potential customers for radiopharmacies interested in distributing

FDG. Obviously most of the departments which owned a SPECT/PET scanner did not have their own cyclotron and were dependent upon delivery of FDG from an outside source. At about the same time the first mobile PET scanners became available. In combination with the first reimbursement in 1998 the stage was set for a large number of nuclear medicine departments to offer PET scanning as a diagnostic tool without the hurdle of a major financial investment and a several year effort to establish a full-blown PET centre including a cyclotron. In the long run dual detector SPECT/PET scanners did not achieve the same diagnostic accuracy as dedicated PET scanners (even if the acquisition time was increased) and simply helped with the transition from a few luminary PET centres to wide-spread availability of PET using distributed FDG.

It is also instructive to look at the early companies which manufactured PET scanners and the significantly different approaches to the market used by each.

CTI started with a design, which originated at Washington University and was first commercialized by Ortec. Ortec became impatient with the slow development of the PET market and allowed a number of its employees to spin the product off into a new company—CTI. CTI's attitude was that they wanted to be the major force in the total PET market and in short order added a cyclotron to their product offering. They also worked closely—and initially primarily—with Universities and emphasized publications. They became a major force in the Institute of Clinical PET (ICP) as a way to promote the field and try to obtain reimbursement instead of working through the Society of Nuclear Medicine.

Scanditronix developed a PET scanner that was an outgrowth of a design, which originated at Karolinska Hospital and they continued to collaborate for years with investigators at Karolinska under the direction of L Eriksson. Scanditronix used a similar strategy to CTI's: they produced a PET scanner primarily for researchers and offered a cyclotron as well, so that they could supply a complete PET centre including the chemistry modules to produce radiopharmaceuticals. However, they did not get involved with reimbursement issues.

UGM Medical Systems started to commercialize the scanner developed as the PENN-PET at the University of Pennsylvania. Their main goal was to develop a clinically useful scanner and they decided to grow with the PET market without trying to directly influence its emergence. As mentioned above, the high start-up cost of a PET centre prevented most nuclear medicine departments from acquiring PET capability. In order to reduce the hurdle to offering PET imaging, UGM—through a technology transfer agreement with ADAC—was instrumental in bringing a dual purpose SPECT/PET scanner to the market.

Finally, Positron Corporation assumed that the major application of PET would be in the cardiac area and they emphasized that market segment. Unfortunately, cardiac PET never became a major application for clinical PET. Positron Corporation was funded largely by venture capitalists, who expected rapid growth and this in combination with a focus on the wrong market segment made Positron Corporation falter for many years.

As so often happens, big companies enter after start-up companies develop the initial product and after the market starts to grow. Thus CTI teamed up with Siemens and was eventually acquired by Siemens, Scanditronix sold the PET scanner part of its business to General Electric and UGM Medical Systems first merged with ADAC, which then itself merged with Philips Medical Systems shortly thereafter. While PET instrumentation is not mature technologically yet, the development has by now largely moved out of University laboratories and small companies to the three major players in diagnostic imaging.

Finally the advent of PET/CT shifted PET from a purely nuclear medicine technique by attracting the attention of radiologists, who sometimes think of PET as a different form of a contrast agent for CT, much to the dismay of nuclear medicine practitioners. The participation

of Radiology departments in the purchase and use of PET/CT scanners has been the most recent cause for increased use of PET scanning as a diagnostic tool.

Time of flight

Overall, today's PET instruments offer good performance for clinical oncology studies. Whole-body scanners have intrinsic spatial resolution that varies from about 4.5–6 mm (fwhm). However, this resolution is not achieved for realistic activity distributions, since in general we do not have sufficient counts to reconstruct the data with a spatial resolution better than 10 mm. Despite the favourable properties of GSO, LSO, LYSO for 3D PET, these systems still suffer from a high fraction of scattered radiation and randoms, particularly for heavy patients as discussed above.

Besides the reduction in randoms and scatter we can further improve the quality of the reconstruction by including the time-of-flight (TOF) information in the reconstruction. The utilization of TOF is known to improve the signal-to-noise ratio in PET images (Budinger 1983), by reducing the noise propagation along the line-of-response (LOR) during the forward- and back-projection steps in image reconstruction. The variance reduction translates to an effective sensitivity gain which has in the past been described simply as a ratio of $D/\Delta x$, where D is the object diameter, $\Delta x = c\ \Delta t/2$, c is the speed of light and Δt is the (fwhm) timing resolution. It is intuitive that the TOF gain is related to this ratio, but not necessarily equal to it. In fact, it is too simplistic to characterize the TOF gain as a single value, since it will certainly be task dependent and must also depend on the method of data correction and image reconstruction. For example, (Tomitani 1981) argued that once reconstruction effects are included, the variance reduction (or sensitivity gain) should be $D/1.6\Delta x$, thus reducing the impact of TOF compared to the simpler estimate given above. For example, for a 27 cm diameter phantom the improvement is approximately 3.8, 1.9 and 1.1 for assumptions of 300 ps, 600 ps and 1000 ps (fwhm) timing resolution using the formula in Tomitami (1981). This implies that the timing resolution needs to be significantly better than 1 ns for TOF to be a benefit for whole-body imaging.

Although the idea of using TOF was originally proposed in the 1960s (Anger 1966, Brownell *et al* 1969, Budinger 1977), it was not until the early 1980s that the first TOF PET systems were built (Ter-Pogossian *et al* 1982, Gariod *et al* 1982, Wong *et al* 1984, Lewellen *et al* 1988, Mazoyer *et al* 1990) using either CsF or BaF_2 scintillators. A good summary of this work, principally from Washington University, CEA LETI, and University of Texas, is included in Lewellen (1998). In general, these early systems used a 1-to-1 coupling of the crystal to PMT, since the low light output of the scintillators and availability of fast timing PMTs did not allow much choice for light sharing and decoding crystals, as is commonly done today. This led to poor packing fraction, particularly with CsF, and poor spatial resolution of about 10–15 mm, since the crystals were large in cross-section (typically 18–24 mm). The final SuperPETT 3000 scanner, however, did use a block decoding scheme (Lewellen *et al* 1992), with improved spatial resolution of about 8 mm. Also, all of these TOF PET systems operated only in 2D mode with multiple (four to five) rings and inter-plane septa and thus had relatively low sensitivity compared to non-TOF scanners using BGO (also 2D), which has higher stopping power than either CsF or BaF_2. On the other hand, intrinsic timing resolution with CsF or BaF_2 is very good, 350 to 440 ps (Moszynski *et al* 1984). Still, losses in the detector and other aspects of the system led to an overall coincidence timing resolution of about 500 to 750 ps, and it was reported to be very challenging to attain this performance on a daily basis due to difficulties with reliability and stabilization of electronics and calibrations. Although these early systems were capable of meeting the high countrate demands of research brain

Table 4. Comparison of coincidence resolving time with $LaBr_3$(Ce) and LYSO(5%Y) which has very similar properties to LSO. Coincidence timing resolution Δt is measured relative to a 2nd identical detector. The single crystal measurement is performed with the crystal directly coupled to a PMT, while the detector measurement incorporates a light-guide to share the light amongst several PMTs required for crystal identification. These are representative measurements using crystals thick enough for PET (20–30 mm) and fast, yet practical PMTs.

Crystal configuration	LaBr (5%Ce) Δt (fwhm) (ps)	LYSO Δt (fwhm) (ps)
Single crystal	250	410
Detector—crystal array	315	650

and heart studies using short-lived isotopes (such as ^{15}O-water), they could match neither the spatial resolution nor the sensitivity of BGO scanners, even with the effective TOF sensitivity gain. By the early 1990s, these early TOF scanners were retired—just before whole-body oncology studies with ^{18}F-FDG became prevalent.

Today, there are new scintillation materials that combine fast timing with high light output, thereby allowing us to overcome the limitations of CsF and BaF_2. The primary candidates are LaBr(Ce) (Surti *et al* 2003), LSO (Moses 2003), and LYSO with similar timing properties as LSO. First results of the performance of TOF PET scanners are reported by several groups, including CTI (Conti *et al* 2005), Donner Laboratory (Moses and Ullisch 2006) and the University of Pennsylvania (Karp *et al* 2006a).

The timing data in table 4 demonstrate that LaBr(Ce), LYSO (and LSO) are good candidates for TOF. Previous problems with packing fraction have been eliminated, since the spacing between crystals is typically only 5–10% of the size of the crystal, thus, good spatial resolution can be achieved using crystals with 4×4 mm^2 cross section and crystal-to-PMT encoding of 50:1 to 100:1 depending on the scintillator. For example, the design of the TOF detector developed at U Penn is based on a pixelated Anger-logic detector using $LaBr_3$(Ce) (Kuhn *et al* 2004), similar in concept to non-TOF detectors that were built previously with NaI(Tl), GSO and LYSO. Also, new digital electronics seems to have solved essentially all of the instability problems plaguing the designs of the 1980s. In summary, TOF PET scanners can now be designed to have all the desirable features and high performance of non-TOF scanners with the added benefit of the TOF image improvement.

Benefit of TOF for 3D PET

A recent demonstration of the benefit of TOF via phantom studies was performed with a LaBr scanner (Karp *et al* 2006a), which uses 38 880 LaBr crystals ($4 \times 4 \times 30$ mm^3) in a cylindrical arrangement with an axial FOV of 25 cm. We performed measurements with two water-filled cylindrical phantoms of diameters 27 cm (vol = 24 l) and 35 cm (vol = 53 l) representing an average and heavy patient respectively. A ring of six spheres with diameters 37, 28, 22, 17, 13 and 10 mm was placed at radial distance of 7 cm in the two phantoms and centred axially in scanner for data acquisition. The two large spheres were 'cold' in all measurements. Figure 5 shows reconstructed images for the two phantoms with 4:1 activity concentration ratio for a 'clinical equivalent' whole-body scan time of 3 min/frame. The smallest 10 mm diameter hot sphere in the 27 cm phantom and the 13 mm sphere in the 35 cm have very low contrast and are at the limit of detectability in the non-TOF image, while TOF image shows better contrast and detectability. Also shown is a transverse section of a patient study from an LYSO scanner (Karp *et al* 2006b) reconstructed both with and without using the TOF information.

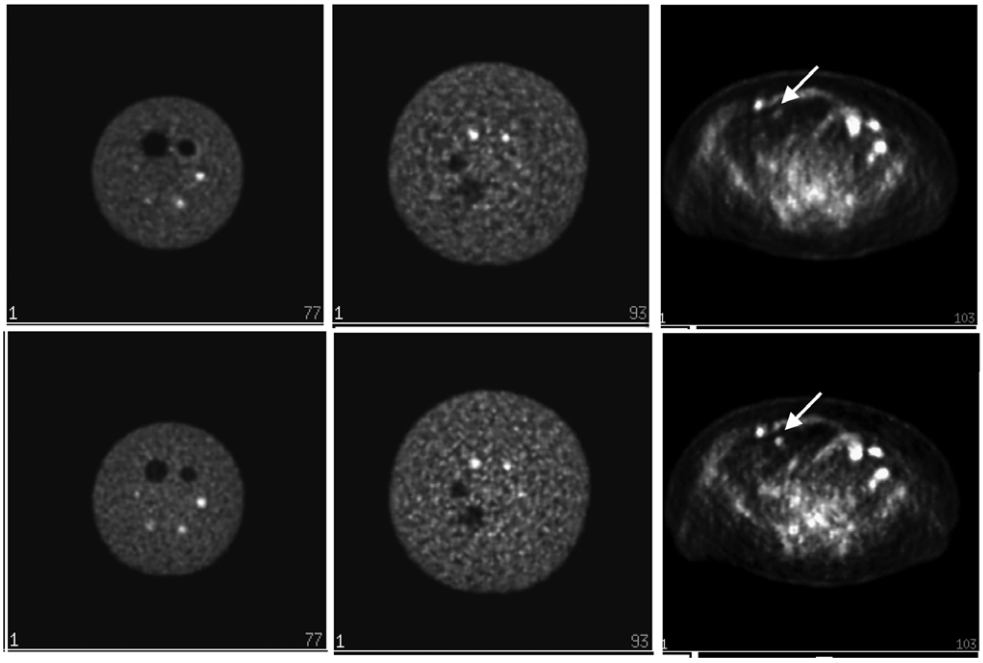

Figure 5. Comparison of measured data reconstructed without (top row) and with TOF information (bottom row). The phantom diameter is 27 cm (left column) and 35 cm (middle column). The timing resolution for these studies is 460 ps (fwhm). The patient images (right column) from a 119 kg patient were acquired in 3 min per frame. The timing resolution for this study is 685 ps (fwhm).

The patient study demonstrates that overall structures are sharper and lesions (see arrow) have higher contrast, in accord with the phantom study.

Dedicated and animal scanners

The story of PET instrumentation development would be incomplete without at least some mention of special purpose PET scanners. High resolution brain scanners, animal scanners and breast scanners deserve particular mention. In all cases the main goal is to achieve better spatial resolution and higher sensitivity than is achieved with general purpose whole-body PET scanners. Using smaller crystals and a smaller detector diameter are obvious methods to improve spatial resolution and sensitivity, although this has required innovative development of new technology for PET. Application of new scintillation crystals, including LSO (Cherry *et al* 1997), and new photodetectors, such as avalanche photo-diodes (APDs) (Lecomte *et al* 1996) and position-sensitive photo-multiplier tubes (PS-PMTs) have been tried first with animal scanners. A nice summary of the development of dedicated animal scanners is given by Chatziioannou (2002), who was part of Simon Cherry's team at UCLA developing the first microPET scanner. The current state-of-the-art in commercial systems typically achieve about 1.5 mm spatial resolution, although there are a number of systems under development that are being designed to achieve better than 1 mm spatial resolution with high sensitivity. Although LSO has found its way to clinical whole-body PET scanners, APDs and PS-PMTs are still too expensive for a large system.

Another innovative technology that has been developed for dedicated scanners is for measurement of depth-of-interaction (DOI). With a smaller detector diameter the angle through

the crystal can lead to mispositioning and loss of spatial resolution at larger radii. To counter this effect a number of investigators have proposed and implemented various, often ingenious schemes to determine the depth of interaction in the crystals. One such technique is the phoswich technique which crystals with different decay time characteristics (Saoudi *et al* 1999), and another technique is to use photo-sensors on both sides of the crystal to share the light, for example a photodiode on the front side and the traditional PMT on the back side (Huber *et al* 1997). So far these schemes are still too complicated to implement them in clinical whole-body scanners in a cost effective way. However, the Siemens HRRT dedicated brain uses DOI with two layers of crystals with different decay times, first configured with LSO and GSO (Schmand *et al* 1998) but later configured with LSO and LYSO, and achieve a spatial resolution of close to 2 mm uniformly over the field-of-view. The group at the National Institute of Radiological Sciences in Japan has implemented a scheme with four layers of crystals for both an animal scanner (Tsuda *et al* 2006) and a brain scanner (Yoshida *et al* 2006).

There has been considerable development in the last few years in animal scanner instrumentation to coincide with increased interest in pre-clinical investigations and development of new radiopharmaceuticals. Certainly it has been demonstrated that PET is capable of providing detailed metabolic images of small animals, giving the investigator the capability to measure and quantify a multitude of novel biochemical activities of different organs and disorders in their natural state. While it might be hoped that high-resolution brain and breast scanners would also find wide-spread application, this has not been the case so far. The primary clinical application of brain scanning is Alzheimer's disease, which shows up as large areas of decreased FDG metabolism and does not benefit significantly from better spatial resolution. For abnormalities other than dementia improved spatial resolution is an advantage, although the therapeutic options for many neurological disorders remain fairly limited. For breast scanning improved spatial resolution helps detect and characterize small lesions but the primary benefit of a dedicated scanner may be improved sensitivity; in fact the scanner sensitivity can be improved by an order of magnitude by using small detectors close to the breast and avoiding the large attenuation due to the body. However, FDG is probably not the right tracer for early breast cancer and wide-spread use of dedicated breast imaging may depend more on availability of a better tracer than a better instrument (Mankoff *et al* 2003).

Summary

If we examine the areas of progress in the last two decades, it becomes clear the there has been only a modest amount of improvement in spatial resolution by decreasing the crystal size (both the *HR-plus* from CTI/Siemens and the *Advance* from General Electric used 4 mm crystals in the transverse direction more than 10 years ago), but there has been significant progress in clinical image quality during the same period. Much of this improvement has come from the combination of iterative reconstruction algorithms, fully 3D acquisition (leading to higher sensitivity) and from good (accurate and low noise) attenuation correction.

A further area of development more recently that has had a major impact has been the replacement of radioactive transmission sources by a transmission CT scan, which not only affected the clinical utility and diagnostic information of PET scans, but also moved PET more into mainstream radiology.

If we look to the clinical need instead of physical scanner parameters, then the image quality of heavy patients and the total scanning time stand out as a major challenge. While TOF scanners are just entering clinical use, it will be probably several years until they are widely available. It can be assumed that over the next few years the timing resolution will continue

to improve and will lead to better image quality for heavy patients and shorter imaging times as well.

PET has taken a long time to move from a research tool to routine clinical use. At the same time, image quality has improved greatly. However, PET imaging is still in a phase of rapid technological development and this is likely going to continue for many years.

References

Alessio M, Kinahan P E, Cheng P M, Vesselle H and Karp J S 2004 PET/CT scanner instrumentation, challenges, and solutions *PET Imaging: I* ed A Alavi Radiol. Clin. North Am. 42 (Philadelphia, PA: Elsevier Saunders) 1017–32

Anger H O 1966 Survey of radioisotope cameras *J. Nucl. Med.* **5** 311–34

Bengel F M, Ziegler S I, Avril N, Weber W, Laubenbacher C and Schwaiger M 1997 Whole-body positron emission tomography in clinical oncology: comparison between attenuation-corrected and uncorrected images *Eur. J. Nucl. Med.* **24** 1091–8

Bohm C, Eriksson L, Bergstroem M, Litton J, Sundman R and Singh M 1978 A computer assisted ring detector positron camera system for reconstruction tomography of the brain *IEEE Trans. Nucl. Sci.* **25** 624–37

Brownell G L, Burnham C A, Wilensky S, Arnonow S, Kaemi H and Strieder D 1969 New developments in positron scintigraphy and the application of cyclotron-produced positron emitter *Medical Radioisotope Scintigraphy (IAEA Proceedings of a Symposium (Salzburg, Austria, August 1968))* (Vienna: IAEA) pp 163–76

Budinger T F 1977 Instrumentation trends in nuclear medicine *Semin. Nucl. Med.* **7** 285–97

Budinger T F 1983 Time-of-flight positron emission tomography——status relative to conventional PET *J. Nucl. Med.* **24** 73–6

Burnham C, Bradshaw J, Kaufman D, Chesler D and Brownell G L 1983 A positron tomograph employing a one dimension BGO scintillation camera *IEEE. Trans. Nucl. Sci.* **30** 661–4

Burnham C A, Bradshaw J, Kaufmann D, Chesler D A, Stearns C W and Brownell G L 1985 Design of a cylindrical shaped scintillation camera for positron tomographs *IEEE Trans. Nucl. Sci.* **32** 889–93

Carson R E, Daube-Witherspoon M E and Green M V 1988 A method of post-injection PET transmission measurements with a rotating source *J. Nucl. Med.* **29** 1558–67

Casey M and Nutt R 1986 A multislice two-dimensional GO detector system for PET *IEEE Trans. Nucl. Sci.* **33** 760–3

Chatziioannou A F 2002 Molecular imaging of small animals with dedicated PET tomographs *Eur. J. Nucl. Med.* **29** 98–114

Cherry S R *et al* 1997 MicroPET: a high resolution PEt scanner for imaging small animals *IEEE Trans. Nucl. Sci.* **44** 1161–6

Cherry S R, Tornai M P, Levin C S, Siegel S and Hoffman E J 1995 A comparison of PET detector modules employing rectangular and round photomultiplier tubes *IEEE. Trans. Nucl. Sci.* **NS-42** 1064–8

Cho Z H and Farukhi M R 1977 Bismuth germanate as a potential scintillation detector in positron cameras *J. Nucl. Med.* **18** 840–4

Cho Z H, Hilal S K, Ra J B, Hong K S, Bigler R E, Yoshizumi T, Wolf A P and Fowler J S 1983 High-resolution circular ring positron tomograph with dichotomic sampling: Dichotom-I *Phys. Med. Biol.* **28** 1219–34

Colsher J G 1980 Fully three-dimensional positron emission tomography *Phys. Med. Biol.* **25** 103–15

Conti M, Bendriem B, Casey M, Chen M, Kehren F, Michel C and Panin V 2005 First experimental results of time-of-flight reconstruction on an LSO PET scanner *Phys. Med. Biol.* **50** 4507–26

Dahlbom M, Hoffman E J, Hoh C K, Schieppers C, Rosenqvist G, Hawkins R A and Phelps M E 1992 Whole-body positron emission tomography: Part I. Methods and performance characteristics *J. Nucl. Med.* **33** 1191–9

Daube-Witherspoon M E *et al* 2002 PET performance measurements using the NU 2–2001 standard *J. Nucl. Med.* **43** 1398–409

Derenzo S E, Budinger T F, Huesman R H, Cahoon J L and Vuletich T 1981 Imaging properties of a positron tomograph with 280 BGO crystals *IEEE Trans. Nucl. Sci.* **28** 81–9

DiChiro G *et al* 1982 Glucose utilization of cerebral gliomas measurement by (18F)fluorodeoxyglucose and positron emission tomography *Neurology* **32** 1323–9

Eriksson L, Bohm C, Kesselberg M, Litton J E, Bergstroem M and Blomqvist G 1985 *Metabolism of the Human Brain Studied with PET* (New York: Raven) pp 33–46

Gariod R, Allemand R, Cormoreche E, Laval M and Moszynski M 1982 The 'LETI' positron tomograph architecture and time of flight improvements *Proc. IEEE Workshop on Time-of-Flight Emission Tomography (Washington University, St Louis, MO)* pp 25–9

Hawkins R A, Maddahi J, Phelps M E, Chilton H M and Hubner K F 1991 Panning and financing a PET center *J. Nucl. Med.* **32** 4 35N–41N

Huber J S *et al* 1997 Characterization of a 64-channel PET detector using photodiodes for crystal identification *IEEE. Trans. Nucl. Sci.* **44** 1197–201

Karp J S *et al* 1991a Performance standards in positron emission tomograpy *J. Nucl. Med.* **32** 2342–50

Karp J S *et al* 2003 Performance of a brain PET camera based on Anger-logic GSO detectors *J. Nucl. Med.* **44** 1340–9

Karp J S, Daube-Witherspoon M E and Muehllehner G 1991b Factors affecting accuracy and precision in PET volume imaging *J. Cereb. Blood Flow Metab.* **11** A38–A44

Karp J S, Kuhn A, Perkins A E, Surti S, Werner M E, Daube-Witherspoon M E, Popsescu L, Vandenberghe S and Muehllehner G 2006a Characterization of a time-of-flight PET scanner based on Lanthanum Bromide *IEEE Nucl. Sci. Symp. Conf. Record* **M04-8** 1919–23

Karp J S, Muehllehner G, He Qu and Xiao-Hong Yan 1995 Singles transmission in volume-imaging PET with a Cs-137 source *Phys. Med. Biol.* **40** 929–44

Karp J S, Saffer J R, Perkins A, Alavi A, Newberg A and Loevner L 2006b Benefit of time-of-flight information for whole-body FDG PET *J. Nucl. Med.* **47** [5] 184

Kuhl D E, Edwards R Q, Ricci A R and Reivich M 1973 Quantitative section scanning using orthogonal tangent correction *J. Nucl. Med.* **14** 196–200

Kuhn A, Surti S, Karp J S, Raby P S, Shah K S, Perkins A E and Muehllehner G 2004 Design of a lanthanum bromide detector for time-of-flight PET *IEEE Trans. Nucl. Sci.* **51** 2550–7

Lartizien C, Comtat C, Kinahan P E, Ferreira N, Bendriem B and Trebossen R 2002 Optimization of injected does based on noise equivalent count rates for 2- and 3-dimensional whole-body PET *J. Nucl. Med.* **43** 1268–78

Lecomte R, Cadorette J, Richard P Rodrigue, Lapointe D, Rouleau D, Bentourkia M, Yao R and Msaki P 1996 Initial results from the Sherbrokke avalanche photodiode positron tomograph *IEEE Trans. Nucl. Sci.* **43** 1952–7

Lewellen T K 1998 Time-of-flight PET *Semin. Nucl. Med.* **28** 268–75

Lewellen T K, Bice A N, Harrison R L, Pencke M D and Link J M 1988 Performance measurements of the SP3000/UW time-of-flight positron emission tomograph *IEEE Trans. Nucl. Sci.* **35** 665–9

Lewellen T K, Miyaoka R S and Kohlmyer S G 1992 Improving the performance of the SP-3000 PET detector modules *IEEE Trans. Nucl. Sci.* **39** 1074–8

Mankoff D A, Dunnwald L K and Kinahan P E 2003 Are we ready for dedicated breast imaging approaches? *J. Nucl. Med.* **44** 594–5

Mazoyer B, Trebossen R, Schoukroun C, Verrey B, Syrota A, Vacher J, Lemasson P, Monnet O, Bouvier A and Lecomte J L 1990 Physical characteristics of TTV03, a new high spatial resolution time-of-flight positron tomograph *IEEE Trans. Nucl. Sci.* **37** 778–82

Mazoyer B, Trebossen R, Deutsch R, Casey M and Blohm K 1991 Physical characteristics of the ECAT 953B/31: a new high resolution brain positron tomograph *IEEE Trans. Med. Imaging* **10** 499–504

Moses W W 2003 Time of flight in PET revisited *IEEE Trans. Nucl. Sci.* **50** 1325–30

Moses W W and Ullisch M 2006 Factors influencing timing resolution in a commercial LSO PET camera *IEEE Trans. Nucl. Sci.* **53** 78–85

Moszynski M, Allemand R, Cormoreche E, Laval M, Odru R and Vacher J 1984 Further study of scintillation counters with BaF_2 crystals for time-of-flight positron tomography in medicine *Nucl. Instrum. Methods* A **226** 534–41

Muehllehner G, Buchin M P and Dudek J H 1976 Performance parameters of a positron imaging camera *IEEE Trans. Nucl. Sci.* **23** 528–37

Muehllehner G and Wetzel R A 1971 Section imaging by computer calculation *J. Nucl. Med.* **12** 76–85

Nutt R 2002 The history of positron emission tomography *Mol. Imaging Biol.* **4** 11–26

Perkins A E, Muehllehner G, Surti S and Karp J S 2003 Performance measurements of a pixelated NaI(Tl) PET scanner *IEEE Trans. Nucl. Sci.* **50** 373–7

Phelps M E, Hoffman E J, Mullani N A, Higgins C S and Ter-Pogossian M M 1976 Design Considerations for a positron emission transaxial tomograph (PETT III) *IEEE Trans. Nucl. Sci.* **23** 516–22

Reivich M *et al* 1979 The [F-18]fluorodeoxuglucose method for the measurement of local cerebral glucose utilization in man *Circ. Res.* **44** 127–37

Saoudi A, Pepin C M, dion F, Bentourkia M, Lecomte R, Andreaco M, Casey M, Nutt R and Dautet H 1999 Investigation of depth-of-interation by pulse shape discrimination in multicrystal detectors read out by avalanche photodiodes *IEEE Trans. Nucl. Sci.* **46** 462–7

Schmand M, Eriksson L, Casey M E, Andreaco M S, Melcher C, Wienhard K, Flugge G and Nutt R 1998 Performance results of a new DOI detector block for a high resolution PET-LSO research tomograph HRRT *IEEE Trans. Nucl. Sci.* **45** 3000–6

Senda M *et al* 1985 Performance characteristics of Positologica III—a whole-body positron emission tomograph *J. Comp. Assist Tomogr.* **9** 940–6

Spinks T J, Jones T, Bailey D L, Townsend D W, Grootoonk S, Bloomfield P M, Gilardi M C, Casey M E, Sipe B and Reed J 1992 Physical performance of a positron tomograph with retractable septa *Phys. Med. Biol.* **37** 1637–55

Stoecklin G 1995 Fluorine-18 compounds *Principles of Nuclear Medicine* (Philadelphia: Saunders) pp 178–94

Surti S and Karp J S 2004 Imaging characteristics of a 3-D GSO whole-body PET camera *J. Nucl. Med.* **45** 1040–9

Surti S, Karp J S, Freifelder R and Liu F 2000 Optimizing the performance of a PET detector using discrete GSO crystals on a continuous lightguide *IEEE Tran. Nucl. Sci.* **47** 1030–6

Surti S, Karp J S, Muehllehner G and Raby P S 2003 Investigation of Lanthanum Scintillators for 3-D PET *IEEE Trans. Nucl. Sci.* **50** 348–54

Ter-Pogossian M M, Mullani N A, Hood J T, Higgins C S and Ficke D C 1978 Design considerations for a positron emission transverse tomograph (PETT V) *J. Comput. Assist. Tomogr.* **2** 539–44

Ter-Pogossian M M, Ficke D C, Yamamoto M and Hood J T 1982 Super PETT I: A positron emission tomograph utilizing photon time-of-flight information *IEEE Trans. Med. Imaging* **1** 179–92

Thompson C J, Yamamoto Y L and Myer E 1979 Positome II: a high efficiency positron imaging device for dynamic brain studies *IEEE Trans. Nucl. Sci.* **26** 583–9

Tomitani T 1981 Image-reconstruction and noise evaluation in photon time-of-flight assisted positron emission tomography *IEEE Trans. Nucl. Sci.* **28** 4582–9

Tsuda T, Murayama H, Kitamura K, Inadama N, Yamaya T, Yoshida E, Nishikido F, Hamamoto M, Kawai H and Ono Y 2006 Performance evaluation of a subset of a four-layer LSO detector for a small animal DOI PET scanner: jPET-RD *IEEE. Trans. Nucl. Sci.* **53** 35–9

Wong W H, Mullani N A, Philippe E A, Hartz R K, Bristow D, Yerian K, Gaeta J M and Ketharnavaz N 1984 Performance characteristics of the University of Texas TOFPET-I PET camera *J. Nucl. Med.* **25** 46–7

Wong W H, Uribe J, Hicks K and Zambelli M 1994 A 2-dimensional detector decoding study on BGO arrays with quadrant sharing photomultipliers *IEEE Trans. Nucl. Sci.* **41** 1453–75

Yoshida E, Kitamura K, Tsuda T, Shibuya K, Yamaya T, Inadama N, Hasegawa T and Murayama H 2006 Energy spectra analysis of the four-layer DOI detector for the brain PET scanner: jPET-D4 *Nucl. Instrum. Methods Phys. Res.* A **557** 664–9

Yu S K and Nahmias C 1995 Single-photon transmission measurements in positron emission tomography using Cs-137 *Phys. Med. Biol.* **40** 1255–66

Biography

Gerd Muehllehner received his PhD in 1966 and since then has been active in the field of nuclear medicine instrumentation for almost 40 years, and has concentrated on PET instrumentation development for the last 30 years. He has worked in both industry (Searle Radiographics, UGM Medical Systems, ADAC and Philips) and the academic environment (University of Pennsylvania). In PET he has concentrated on the development of fully 3D scanners for clinical applications. He is now retired but continues to work part-time with J Karp on time-of-flight instrumentation.